

Condition assessment of structures using smartphones: a position independent multi-epoch imaging approach.

Rolands Kromanis¹ and Haida Liang¹

1 Nottingham Trent University, UK, rolands.kromanis@ntu.ac.uk;
haida.liang@ntu.ac.uk

Abstract

Applications of vision-based technologies are becoming more prevalent in deformation monitoring of civil structures, especially bridges. Feature recognition, detection and tracking algorithms are developed to analyse structural response. For example, movements of structural features such as bolts in steel bridges can be tracked when a truck crosses a bridge. In order to measure small structural movements, good quality and high resolution images are needed. Developments in smartphone technologies have resulted in very good quality on board cameras. Bridge inspectors could use smartphone technologies during visual inspections as they are readily available. Cameras have been used in structural deformations monitoring, however, the challenge is to make sure that the camera is placed in the same location to allow accurate comparison. This study explores if multi-epoch imaging approach can be used to collect accurately structural displacements when capturing images of a structure from different positions. A laboratory beam served as a testbed. Smartphones placed at different positions were used to capture deformations of the beam in healthy and damaged states. Structural feature were selected, and their location were estimated from images. Feature locations from all smartphones were transformed to the reference coordinate system as derived from one smartphone. Results show that feature locations can be accurately transformed to the reference coordinate system, from which difference between undamaged and damaged states of the beam can be recognized.

1. Introduction

Main drivers affecting bridge performance are large traffic loads and environmental effects such as continuously changing ambient temperature to which bridges are regularly exposed (1). In order to assure that bridges are safe to use and fit for purpose while being subjected to the variety of loadings, general (visual) inspections in the UK are carried out every two years (2). Visual inspections are frequently subjective and rely on inspectors' decisions (3). This subjectivity can be minimised, when structural response to known loads is measured. Sensor systems can be deployed to monitor and learn about the bridge performance and support asset management. Conventional sensor systems consist of contact sensors and data acquisition and transmission units. Their installation is usually difficult involving risks related to the access of sensor locations and working at heights and causing traffic disruptions (4). These could be minimized significantly using non-intrusive laser- or vision-based technologies such as cameras (5).

Today vision-based systems are becoming more prevalent than years ago. However, challenges that need to be addressed before they become robust, reliable and ubiquitous still remain. Main challenges involve an estimation of accurate engineering



measurements, a provision of a fixed position of the camera and variation of lighting (6). An important factor to consider when deciding to employ cameras in long-term continuous monitoring are temperature variations which cause large measurement errors (7). Furthermore, the provision of stable and secure locations, robust cameras and online data access is needed. Another option is to carry out short-term static load tests, in which a truck with a known weight such as an AASHTO HS-20 design truck, is driven over the bridge (8). In this scenario, thermal effects can be neglected and the bridge under loading can be monitored using stationary cameras or unmanned aircraft system (9, 10). Structural response such as vertical or total displacements can be estimated from collected images or recorded videos in real-time.

Static and dynamic bridge response could be measured during visual bridge inspections. Such information would be less subjective to human errors and could be compare with measurements obtained from previous inspections. The load-response chain would only change if the structure was damaged or previously unseen loads were applied, such as during the maintenance. In past years, smartphone technologies with their embedded cameras and supporting software have developed rapidly. For example, Samsung S9 can record ultra-high-definition 4k (3840 x 2160 pixel) videos at 60 frames per second and high-definition (1280 x 720 pixel) videos at 960 frames per second. Smartphones have the capability to capture images comparable to professional cameras, therefore broadening their applications and opening opportunities to explore them in the structural monitoring field.

The premise of this study is that relationships between multiple structural features such as bolts in cast iron bridges remain the same even when images of the structure are taken from different angles. The assumption is made that these features are located on the same structural plane. This study employed smartphone technologies to investigate (i) if the location of structural features could be accurately located from images collected at different angles, (ii) if structural response could be accurately estimated (iii) and if measured response is accurate enough to detect damage. A timber beam with artificially drawn structural features served as a testbed. The beam was subjected to static load tests in healthy and damaged conditions. While the beam was undergoing load tests, smartphones were used to collected images, from which marker locations were obtained and transformed to the selected reference plane.

2. Position independent multi-epoch imaging approach

When measuring structural response of a bridge using vision-based technologies some assumptions and estimations have to be made to find a converting ratio, which can be used to express pixel values to world units. The most common practice is to use a checkerboard, which has black and white squares with known dimensions, to derive a converting ratio. It is also possible to use the size of a known element such as bolt or structural section. These methods work well when collecting static and dynamic structural response over a period of few hours where the camera can be left at the same position (11). But if response needs to be collected periodically, say every months, placing a camera at the exactly same location and assuring that it captures the exact extends of the structure is very challenging. Furthermore, the specification of object

boundaries or known distance, which was used previously (unless a permanent checker boards was installed), might also become challenging.

This study proposes a camera position independent approach for vision-based measurement collection and analysis. This section describes the methodology employed to collect accurate bridge response measurements from different camera positions. Images of an entire structure or a part of it are collected for condition assessment. A set of structural features is selected. Their movements are measured when known loads are applied. It is assumed that these features are located on one plane to avoid parallax effect.

2.1 Laboratory validation assumptions

The proposed multi-epoch image collection approach was validated using a laboratory structure, which was tested in both undamaged and damaged conditions. In real-life scenario, one smartphone could be used during inspections. However, in order to obtain reliable and comparable measurements, in this study, three smartphones were employed to collect images of the laboratory structure, which is a cantilever beam (see Figure 1). One smartphone was used to generate reference data. This is thought to be the first time when the structure is inspected. The other two smartphones were used to validate if similar data can be obtained from different positions. These could be positions of smartphones in the next inspections. Locations of selected structural features are extracted from the images. In this study, artificial markers are considered as structural features, however, in real-world structures, bolts or surface patterns can be chosen. Locations of markers were derived using Deformonit, which is an image processing freeware developed at Nottingham Trent University (NTU) by R Kromanis (12).

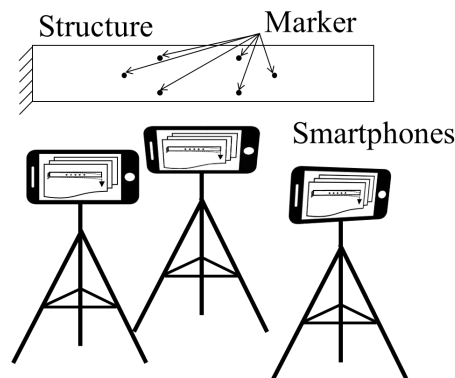


Figure 1. Position independent measurement approach.

To validate the proposed approach, marker coordinates obtained from a reference smartphone are used to generate a transformation matrix that transforms marker coordinates estimated from images collected with other two smartphones to the reference coordinate system. The accuracy of the marker transformation is tested on marker locations that are not included in the generation of the transformation matrix. For illustrative purposes, consider that two smartphones capture a part of the beam (from Figure 1) with artificial markers on its surface. The smartphones are set at different angles to the beam. A closer view of the captured images is shown in Figure 2. The coordinates obtained from both images are derived using an image processing

algorithm. Marker locations from the image shown in Figure 2 (a) are selected to define reference plane/coordinate system. Control points from both sets of marker locations are selected and a transformation matrix is generated. The matrix is then used to transform marker locations obtained from the image in Figure 2 (b) to the reference coordinate system. The deviation (D) between the reference (R) and transformed (T) location of i^{th} marker (M_i) are used to evaluate the accuracy of transformation matrix (see Equation 1). D is expressed in terms of pixel values.

$$D_{M_i} = \sqrt{(x_{M_i,R} - x_{M_i,T})^2 + (y_{M_i,R} - y_{M_i,T})^2} \quad (1)$$

where x and y are coordinates of M on x and y axes.

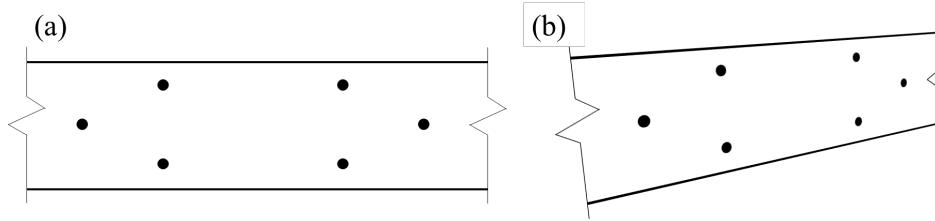


Figure 2. Marker coordinate transformations approach: (a) and (b) part of the structure shown in Figure 1 as captured with different smartphones.

3. Damage detection from structural feature locations

The damage detection approach proposed in this study consists of two phases: identification of baseline conditions and condition assessment (see Figure 3). In both phases images of a structure under static loads such as crossings of heavy vehicles are collected and processed. In the first phase baseline conditions indicating the current state of the structure are identified. In static tests, load-response relationship can be considered. The axle loads of a vehicle can be measured with weigh-in-motion sensors (13). Structural response such as vertical deformations are estimated analysing images that are taken while vehicles cross the bridge. Structural features such as bolts or steel joints are selected. Their locations in a two-dimensional coordinate system (image frame) are estimated for no load periods and periods when loads are applied. In the second phase, which is repeated as frequently as required, the load-response relationship is estimated similarly to the identification of baseline conditions phase. The only difference is that the locations of features are compared against baseline conditions. This is common and frequently used practice when contact sensors are employed (14). However, when considering vision-based systems, locating a camera in exactly the same place where it was located at the collection of images for the baseline conditions is a challenging task. This, however, is dealt with using the proposed multi-epoch image collection approach.

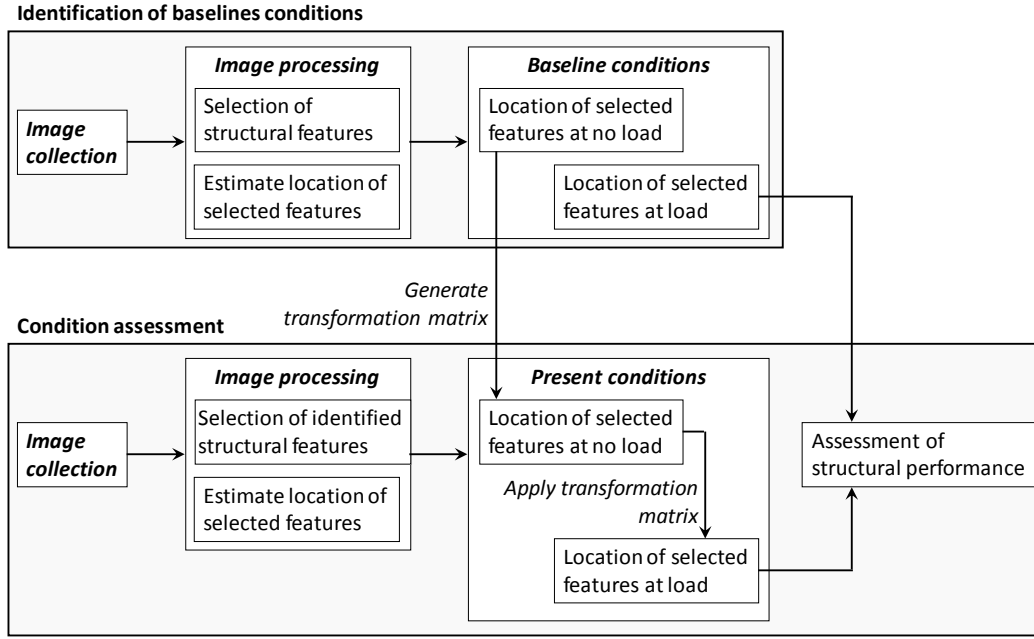


Figure 3. Multi-view measurement collection and analysis approach.

In this study the structure was tested in both healthy and damaged states. The difference of the marker displacements are compared. If displacements of markers vary from baseline conditions when the beam is subjected to the same load, damage is detected. In this study the marker displacement in vertical and horizontal axes are converted to total displacement which is considered as a damage sensitive feature. Total displacement (δ) at i^{th} marker for j^{th} smartphone (S) is calculated from estimated marker coordinates at load (L) and no load (N) conditions as follows:

$$\delta_{M_i, S_j} = \sqrt{(x_{L, M_i, S_j} - x_{N, M_i, S_j})^2 + (y_{L, M_i, S_j} - y_{N, M_i, S_j})^2} \quad (2)$$

4. Laboratory tests

A laboratory testbed was set-up in the structures laboratory at NTU. Coordinates of artificial markers of the testbed were obtained when no load and load were applied to the beam in undamaged and damaged conditions. Structural response estimated from marker locations were analysed for damages.

4.1 Laboratory test set-up

A timber cantilever beam served as a testbed for this study. The beam was 950 mm long, 45 mm wide and 70 mm high (see Figure 4). Multiple artificial markers were drawn on its surface, out of which 10 markers were selected to obtain beam deformations and validate the proposed structural condition assessment approach. Beam deformations were collected during a static load test in which the beam was in healthy and damaged conditions. 100 N load was manually applied at the free end of the beam. Damage was created by removing a 40 mm timber block from the bottom (tensile side) of the beam. The centre of the block was located 465 mm from the beam support.

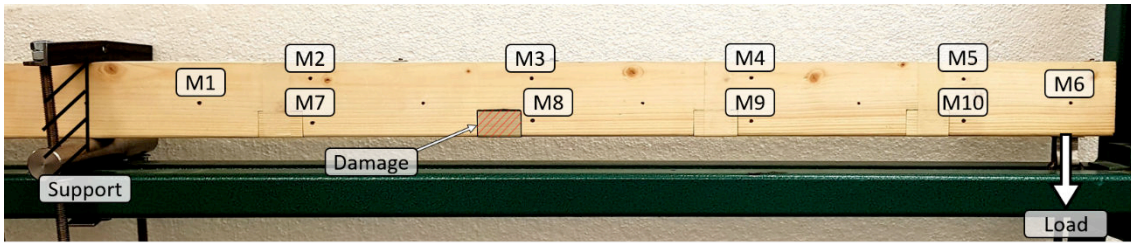


Figure 4. Laboratory beam supported at the left end and loaded on the right end. Markers (M_i , where $i=1, 2, \dots, 9$) were drawn on the surface facing the camera. The rectangular area hatched in red represents the damage location.

Three smartphones were used to obtain beam deformations (see Figure 5). Images were taken at a rate of 1 frame per second. The first images of the undamaged beam collected with all smartphones are shown in Figure 6. S1 (Samsung A3) and S2 (Samsung A5) were located at the same height as the beam (Figure 6 (a) and (b)) allowing to capture the front view from a slightly different angle. Figure 6 (c) shows a projective view of the beam, in which the right end of the beam looks as if it was larger than the left end. This image was captured with S3 (Samsung S8). The first image collected with S1 was selected as the reference image. It is used to derive marker locations representing structural plane.

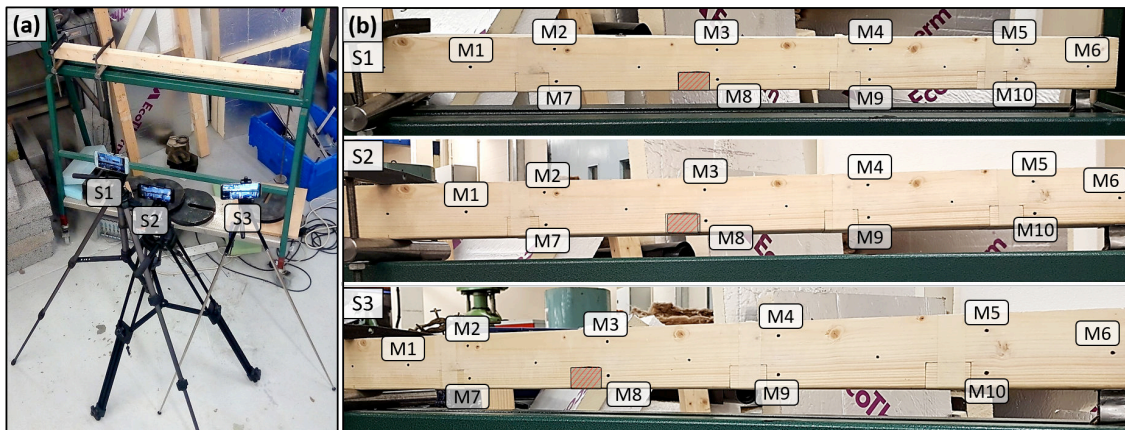


Figure 5. Timber beam at no load: (a) location of smartphones (S_j , where $j = 1,2,3$), (b) images collected with S1, S2 and S3.

4.2 Verification of marker transformation

In total 10 markers were chosen and selected in all images. Their locations on x and y axes were calculated using image processing analysis. Four pairs of widely distributed control points (reference points and points that need to be transformed to the reference coordinate system) are selected to generate a transformation matrix. To evaluate the performance of the transformation matrix, the total error between reference points and transformed points are computed for points that were not used to derive the transformation matrix.

The smallest prediction errors for S2 and S3 were obtained using M1, M2, M5 & M9 and M1, M5, M8 & M10 respectively as control points. The marker locations obtained for the combination of the listed markers were used in later sections. The minimum and

maximum pixel errors for S2 and S3 were 2.0 & 1.8 pixel and 6.0 & 11 pixels respectively. The accuracy of the matrix transformation can be attributed to the accuracy of the derived marker locations. The centre of the marker (blob) is used as the marker location. The centre of a particular marker might be calculated at a slightly different location in images taken from different angles or different light conditions. This factor needs further investigation and, for the reasons of brevity, is not included in this paper.

4.3 Structural response

Total displacements of markers (see Equation 2) when the undamaged beam is subjected to the load are shown in Table 1. The values are obtained from the image taken with S1. The total displacement of markers located farther from the beam support is larger than that of the markers located closer to the support. This was expected for a cantilever beam.

Table 1 Total marker displacements as estimated from images taken with S1 when the load is applied to the beam

| | M1 | M2 | M3 | M4 | M5 | M6 | M7 | M8 | M9 | M10 |
|--------------------------|-----|-----|-----|----|----|----|-----|-----|------|-----|
| δ_{T,S_1} [pixel] | 1.3 | 2.5 | 5.8 | 10 | 16 | 19 | 2.2 | 5.7 | 10.3 | 16 |

The plot of all marker locations are shown in Figure 6 (left). Overall, transformed marker locations match well with the reference marker locations. Figure 6 (right) shows a closer look at M4 location. Location of M4 has the highest deviation from the reference marker for both S2 and S3 (see Figure 7). Calculated M4 locations do not coincide, however, there is a trend between the locations at no load and load conditions. As mentioned previously, such deviations can be attributed to the differences arising when determining the centre of a marker in the image processing phase. This is explained in Figure 7, where deviations between marker locations estimated from S1 images and S2 & S3 images are derived. The bar graph shows that total deviations for marker locations for no load and load conditions are smaller than 5.5 pixels for S2, however, deviations obtained from S3 are as high as 11 pixels.

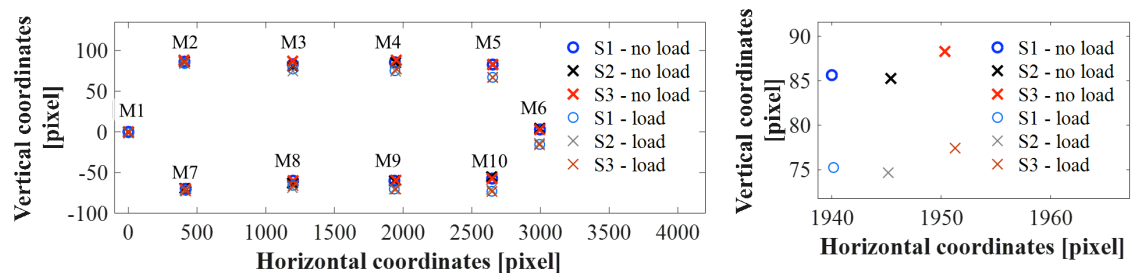


Figure 6. Plot of all marker coordinates (left) and a closer look at M4 coordinates (right) obtained from all smartphones with and without load.

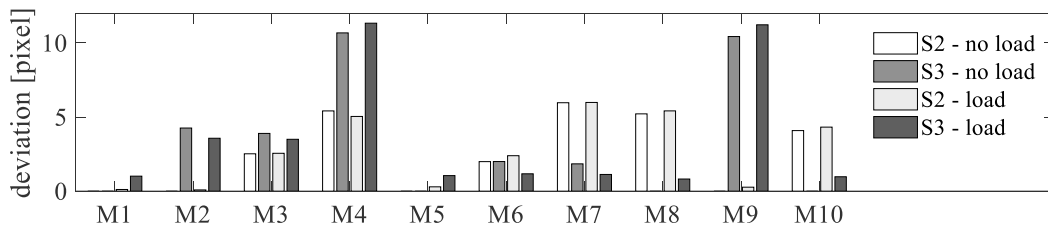


Figure 7. Bar plot of pixel deviations between S1 and S2 & S3 for no load and load states of the beam.

4.3 Damage detection

Time histories of M9 total displacements obtained from images collected with all smartphones and calculated after transforming marker location to the reference coordinate system are shown in Figure 8. Measurement peaks represent periods when loads were applied. A slight change in displacements can be observed when looking at two peaks. This indicates the increase of total deformation after the beam was damaged. The deviation between total displacements of reference and transformed markers were considered as damage sensitive feature.

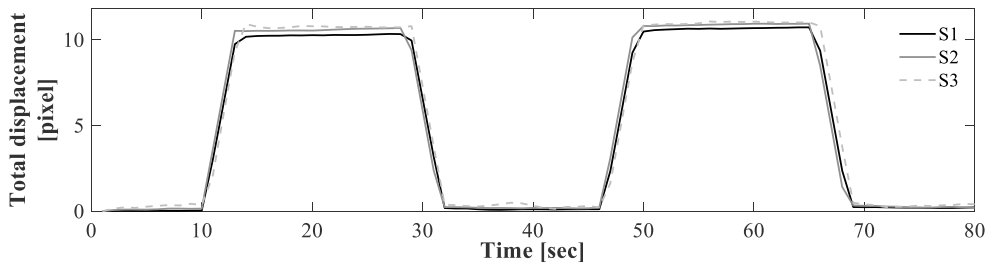


Figure 8. Time histories of total displacements for M9.

The total displacement for each marker when the beam was subjected to loading while being in both healthy and damaged states are showing in Figure 9. Total displacements of markers to the left of the damage – M1, M2 and M7, were not expected to be affected when the beam was damaged. From the total displacements obtained from S2 and S3 the damage cannot be reliably located without prior knowing of the damage location. Sums of total deviations for (i) S2 and S3 in undamaged and damage scenarios are 1.3 pixels & 2.9 pixels and 3.5 pixels & 5.1 pixels respectively and (ii) S1 in damaged scenario is 2.3 pixels. The sum of deviations of the undamaged beam as calculated from S2 is 1.3 pixel versus 2.3 pixel of damaged beam calculated from S1. This alone might raise false alarms suggesting that other damage sensitive parameters such as strains and tilts could be derived from marker locations to assess structural conditions.

When comparing total displacements of undamaged and damaged beam as captured with S1, large deviations are found for M4, M5, M6, M9 and M10. These markers are located to the right of the damage location (away from the support). M8 is right next to and M3 is just above the damage location, however, total displacement values for these markers are small and deviations between these values are almost negligible.

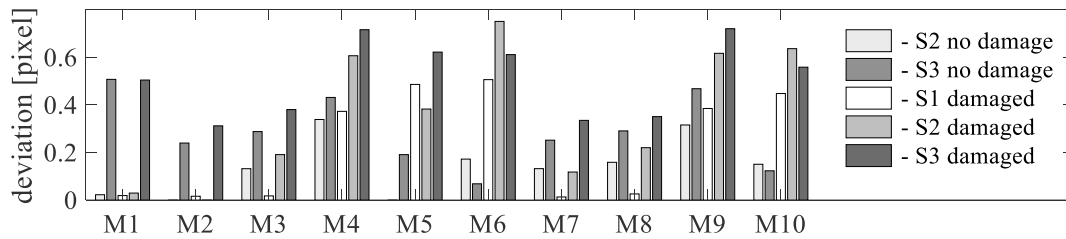


Figure 9. Deviations of total displacements between S1 and S2 & S3 for healthy and damaged states of the beam subjected to loading.

Overall, the experimental tests provided a good insight in problems that have to be addressed before the multi-epoch image collection approach can be adapted for the condition assessment of full-scale structures. Deviations of marker locations from one camera to another camera can be related to the way the marker coordinates were computed from images. The selected image processing freeware (Deformonit) analyses a user specified region of interest within which lies a marker. The centre of the blob is calculated using maximally stable extremal regions algorithm. The centre of a marker might be estimated at a slightly different location when analysing images that are captured from different camera positions. Another algorithm or method could be employed to validate if the centre of markers can be accurately identified. To determine structural damage, it is also important to consider the deviation with or without load for a range of widely distributed markers.

5. Conclusions

This study introduced a smartphone application for damage detection from static load tests using a position independent imaging approach. The premise is that the selected structural features are located on one plane and their locations viewed from different positions can be reconstructed using matrix transformation. The ideal was demonstrated on a cantilever beam on which artificial markers were drawn. In real-world bridges, these could be bolts or any other structural features. Results demonstrated that:

- Accurate transformation matrices were generated when selecting four widely distributed control points. With some exceptions, marker locations of the transformed markers were close to locations of reference markers.
- Total deviations between reference and transformed marker locations for no load and load conditions remained fairly similar even for transformed markers having large (10 pixel) deviations from the reference markers. This suggests that deviations between reference and transformed marker locations might be attributed to calculations that were used to estimate the centre of markers.
- Damage can be detected when comparing S1 and S2 results, especially, when looking at sums of total deviations. However, damage location can only be identified when analysing total displacements derived from images collected with S1.

Future studies should evaluate the accuracy of image processing algorithm to estimate correctly the location of structural feature. This could be done on a testbeds with many idealized artificial features that are drawn at known distances or using grids.

Acknowledgements

This project was funded by NTU Global Heritage Section.

References

1. Catbas FN, Susoy M, Frangopol DM. 2008. Structural health monitoring and reliability estimation: Long span truss bridge application with environmental monitoring data. *Eng. Struct.* 30(9):2347–59
2. Road Liason Group. 2005. Management of Highway Structures. London
3. Brownjohn JMW. 2007. Structural health monitoring of civil infrastructure. *Philos. Trans. R. Soc. a-Mathematical Phys. Eng. Sci.*, pp. 589–622
4. Jahanshahi MR, Masri SF, Sukhatme GS. 2011. Multi-image stitching and scene reconstruction for evaluating defect evolution in structures. *Struct. Heal. Monit.* 10(6):643–57
5. Khan SM, Atamturktur S, Chowdhury M, Rahman M. 2016. Integration of structural health monitoring and intelligent transportation systems for bridge condition assessment: Current status and future direction. *IEEE Trans. Intell. Transp. Syst.* 17(8):2107–22
6. Xu Y, Brownjohn JMW. 2017. Review of machine-vision based methodologies for displacement measurement in civil structures. *J. Civ. Struct. Heal. Monit.*
7. Zhou HF, Zheng JF, Xie ZL, Lu LJ, Ni YQ, Ko JM. 2017. Temperature effects on vision measurement system in long-term continuous monitoring of displacement. *Renew. Energy.* 114:968–83
8. Saydam D, Frangopol DM. 2011. Time-dependent performance indicators of damaged bridge superstructures. *Eng. Struct.* 33(9):2458–71
9. Feng D, Feng MQ. 2017. Experimental validation of cost-effective vision-based structural health monitoring. *Mech. Syst. Signal Process.* 88:199–211
10. Gillins MN, Gillins DT, Parrish C. 2016. Cost-Effective Bridge Safety Inspections Using Unmanned Aircraft Systems (UAS). *Geotech. Struct. Eng. Congr. 2016*, pp. 1931–40
11. Khuc T, Catbas FN. 2017. Computer vision-based displacement and vibration monitoring without using physical target on structures. *Struct. Infrastruct. Eng.* 13(4):505–16
12. Kromanis R, Al-Habaibeh A. 2017. Low cost vision-based systems using smartphones for measuring deformation in structures for condition monitoring and asset management
13. Mimbela LEY, Klein LA. 2000. Summary of vehicle detection and surveillance technologies used in intelligent transportation systems
14. Kromanis R, Kripakaran P. 2017. Advanced Engineering Informatics Data-driven approaches for measurement interpretation: analysing integrated thermal and vehicular response in bridge structural health monitoring. *Adv. Eng. Informatics.* 34:46–59